Three-Fragment Counterpoise Correction of Potential Energy Curves for Proton-Transfer Reactions

Alessandro Ponti*,† and Massimo Mella‡

Istituto di Scienze e Tecnologie Molecolari, Consiglio Nazionale delle Ricerche, via Golgi 19, 20133 Milano, Italy, and Dipartimento di Chimica Fisica ed Elettrochimica, Università degli Studi di Milano, via Golgi 19, 20133 Milano, Italy

Received: March 17, 2003; In Final Form: May 27, 2003

We present a thorough study of the effect of basis set choice and of the three-fragment counterpoise correction for the basis set superposition error on the shape of proton-exchange energy surfaces. This has been investigated by employing the correlated MP2 method and basis sets from cc-pVDZ to aug-cc-pVTZ quality. To understand the effect of the correction and the overall accuracy of the different atomic basis sets, and to discover the best-compromise basis set for large surface scans, we computed the shape difference function between corrected and uncorrected results for the HF_2^-, $H_3O_2^-$, $H_5O_2^+$, $N_2H_5^-$, and $N_2H_7^+$ systems. Our results show this function to strongly depend on the system, although larger corrections are consistently observed when the more basic fragments (NH_2^- and OH^-) are involved. Suggestions on which basis set could be used for potential energy surface scans are also given.

Introduction

Proton transfer and proton exchange are ubiquitous in nature. These are involved in processes which range in complexity from "simple" acid−base chemistry up to the catalytic activity of the enzymes. Also, proton transfer from water solution to carboxylate groups seems to be involved in the early steps of protein refolding[1] and denaturation.[2] For these reasons, an understanding of the mechanism underlying proton exchange is needed in many branches of chemistry, and its importance can be hardly overestimated. Notwithstanding such an importance, this mechanism still appears to be not completely understood, and many experimental and theoretical efforts have been carried out. To theoretically elucidate the various steps involved in proton exchange, we believe that two fundamental ingredients are needed. First, the potential energy surface (PES) over which the process takes place must be accurately computed. This would allow one to clarify the energetics of the process as well as to shed some light on the different pathways involved. Second, an accurate, truly quantum-mechanical simulation of the proton behavior is needed. This last requirement has just become mandatory after the suggestion that the thermally excited vibrational state of the proton donor species can play a role in water autoionization[3] and, perhaps, in proton transfer when high barriers separate reactants from products. Moreover, the topology of the PES usually changes from a monostable surface to a bistable one (see for instance ref 4) upon changing the center of mass distance between the donor and acceptor molecules. If so, a strong coupling between the proton motion and the relative motion of the two fragments should be expected, and the use of a quantum-mechanical method is mandatory.[5]

As to the PES, the ideal approach would require the use of correlated ab initio methods to accurately compute "on the fly" energy and energy gradients during a quantum-mechanical simulation. Unfortunately, this task is, at the present, unfeasible unless one resorts to density functional theory as the electronic structure calculation method.[6−8] However, even with this choice, simulation time can hardly span more than a few picoseconds. So, if statistically accurate quantities are sought (e.g., exchange rates and thermodynamic functions), one is forced to resort to a model potential to describe the system.[4,9−11] Often, these model potentials are built starting from physically motivated parametrized terms, and the parameters are optimized by fitting the results of accurate supramolecular ab initio calculations. In this respect, it is now clear that one must always correct the supramolecular interaction energy value in order to minimize the basis set superposition error (BSSE), unless an exceedingly large basis set is used. Although various schemes have been proposed in the past to tackle this issue, the most widespread method is still the counterpoise (CP) correction.[12] Not representing a definitive answer to the difficulties created by the BSSE, CP is nevertheless a viable and effective way to approach this problem.[13] Also, CP gives the "exact" answer in the complete basis set (CBS) limit; i.e., the correction decreases to zero while the atomic basis set becomes complete, and an extrapolation procedure could be devised. The CP correction is usually applied in studies of weak molecular interactions where the molecules can be considered as separate entities whose geometry changes only slightly due to the intermolecular interaction. In contrast, during a proton-exchange step, major changes in both the electronic and nuclear structure take place, and this hinders the possibility to use CP as it is. However, recently a way to correct for the absence in the usual CP approach of the fragment deformation energy has been proposed.[14,15] This is accounted for by computing the difference between the energy of an isolated fragment in its own minimum geometry, and the energy of the same fragment at the geometry in the complex.

* To whom correspondence should be addressed. Phone: +39 02 5031 4280. Fax: +39 02 5031 4300. E-mail: alessandro.ponti@istm.cnr.it.
† Consiglio Nazionale delle Ricerche.
‡ Università degli Studi di Milano. Present address: Central Chemistry Laboratory, Department of Chemistry, University of Oxford, South Parks Road, OX1 3QH Oxford, UK.

10.1021/jp034682z CCC: $25.00
Published on Web 08/20/2003

Another difficulty in applying the CP procedure in describing a proton-exchange process is the fact that it is problematic to designate which molecular fragment the proton belongs to. This makes the selection of which basis functions belong to a given fragment, the first step in the CP procedure, somewhat arbitrary. Luckily, it seems possible to circumvent this difficulty by means of a three-fragment extension of the CP procedure that has recently been proposed.[16,17] In this method, the transferred proton is considered as a fragment by itself with its own basis set. The choice implies a different treatment for the exchangeable proton than for the "fixed" ones if any is present (e.g., the four water protons in $H_5O_2^+$). Nevertheless, it has been found[16] that this procedure introduces only small differences in both the equilibrium geometry and the proton affinity of the protonated isolated fragment when compared with the same quantities obtained without correction but with a good quality basis set.

Using such a procedure, in ref 16 attention has been paid mostly to the characterization of the minima of the PES for $H_5O_2^+$, $H_3O_2^-$, and $NH_4^+H_2O$ employing various basis sets. Conversely, no effort has been devoted to study the effect of such a procedure on the overall topology of the surface and on the height of the potential barrier separating reactants from products. Therefore, we feel that it is important to test the performance of the many-body decomposition and the effect of introducing the fragment relaxation energy for various representative systems. This represents a mandatory step before proceeding to compute the proton-exchange PES with any ab initio method and fitting the results with an adequate analytical form. With this aim in mind, we chose HF_2^-,[18−22] $H_3O_2^-$,[23−27] $H_5O_2^+$,[10,28−31] $N_2H_5^-$,[7,32] and $N_2H_7^+$ [33−35] as representative systems. All these systems have been previously studied with different degrees of sophistication, $H_5O_2^+$ being perhaps the one whose properties have been most extensively scanned. However, for the remaining ones, accurate information on the behavior of the proton-exchange PES including BSSE correction is still scarce, so it also appears interesting to explore their energetics.

The outline of the paper is as follows. First, we summarize the theoretical background of the counterpoise correction to the basis set superposition error and detail our calculations. The next section is devoted to presenting and discussing the results for the various systems under study. Finally, the conclusions drawn from the above results are reported.

Theoretical Background

In this section, the theoretical aspects of the counterpoise (CP) correction of the basis set superposition error (BSSE) are briefly summarized. We begin by considering the simplest case, i.e., the formation of complex AB from the isolated fragments A and B. First, a few concepts are defined at the complete basis set (CBS) limit. In the supramolecular approach, the formation energy ΔE of complex AB from the isolated fragments A and B is given by

$$\Delta E = E_{AB}(AB) - E_A(A) - E_B(B) \qquad (1)$$

where $E_Y(X)$ is the energy of species X at the equilibrium geometry of species Y. Note that eq 1 is valid only if the computational method is size-consistent. With reference to the diagram in Figure 1, the formation energy can be decomposed as follows:

$$\Delta E = \underbrace{E_{AB}(AB) - E_{AB}(A) - E_{AB}(B)}_{E_{app}} + \underbrace{E_{AB}(A) + E_{AB}(B) - E_A(A) - E_B(B)}_{E_{def}} \qquad (2)$$

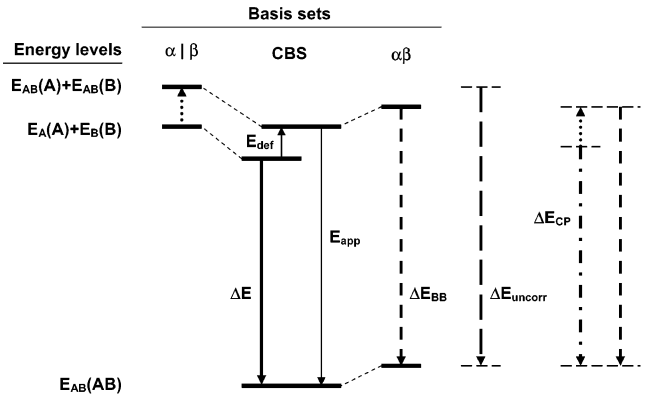

Figure 1. Pictorial representation of the energies involved in the counterpoise correction of the basis set superposition error. The complete basis set (CBS) limit formation energy ΔE is shown (thick arrow), along with its decomposition in deformation and approach energies (thin arrows). Under the heading $\alpha|\beta$, the finite basis set approximation to the deformation energy is shown (dotted arrow). These energy levels, computed using separately the basis sets of fragments A and B, are involved in the definition of the uncorrected formation energy ΔE_{uncorr} (long-dashed arrow). Under the heading $\alpha\beta$, the original Boys−Bernardi formation energy ΔE_{BB} is shown (short-dashed arrow). Note that here a deformation energy cannot be defined. At the far right one can find the counterpoise-corrected formation energy ΔE_{CP} (dash−dotted arrow) as now used. Its decomposition as $\Delta E_{CP} = \Delta E_{BB} + E_{def}$ is also shown.

where the deformation energy E_{def} is the energy needed to deform the fragments from their equilibrium geometry to the geometry they assume in the complex, and the approach energy E_{app} is the energy change due to the rearrangement of the electron density when the two deformed fragments are brought together to form the complex. Clearly, E_{def} is always nonnegative (it vanishes for atoms) and E_{app} is usually negative.

Of course, when real calculations are performed, one is restricted to finite, incomplete basis sets. Within this limitation, the simplest definition of formation energy is

$$\Delta E_{uncorr} = E_{AB}^{\alpha\beta}(AB) - E_A^{\alpha}(A) - E_B^{\beta}(B) \qquad (3)$$

where the greek superscripts denote that the energy of fragment A is computed with its own basis set (the same for B), and the complex energy is computed with the basis set resulting from merging the basis sets of A and B. At the CBS limit, both the α and β basis sets are complete, and eq 3 correctly reduces to eq 1, as shown in Figure 1. However, it is now widely recognized that ΔE_{uncorr} is too negative because the complex energy is computed with a larger basis set than the fragments are. This is the BSSE, which can be corrected following the counterpoise technique proposed by Boys and Bernardi,[12] by evaluating the formation energy as

$$\Delta E_{BB} = E_{AB}^{\alpha\beta}(AB) - E_{AB}^{\alpha\beta}(A) - E_{AB}^{\alpha\beta}(B) \qquad (4)$$

where the fragments' energy is computed with the merged basis set at the geometry the fragments have in the complex. In eq 4, all energies are computed within the same functional space and can be directly compared. However, as can be seen from eq 2 and in Figure 1, ΔE_{BB} does not tend to ΔE at the CBS limit; rather, it tends to E_{app} because of the neglect of the deformation energy. Although the latter was not large in the first application of the CP correction scheme, it was subsequently appreciated that the deformation energy should be reinstated in the expression of the formation energy,[36] so that it converges to ΔE at the CBS limit. The problem now arises of how the deformation

energy should be computed with finite basis sets. The deformation energy cannot be rigorously computed with the joint basis set since one does not know where the basis functions of, e.g., B should be centered when computing $E_A^{\alpha\beta}(A)$.[37] Thus, any expression of the formation energy including the deformation energy contains energy terms computed with different basis sets. Since the CBS limit does not depend on the finite basis set actually employed, one is free to choose the most appropriate basis set and, in principle, computational method. Notwithstanding this freedom, it seems that the most widespread choice is to use the same computational method and the individual fragment basis sets.[14−17,36,38−40] We therefore arrive at the following expression for the formation enery of the complex:

$$\Delta E_{CP} = E_{AB}^{\alpha\beta}(AB) - E_{AB}^{\alpha\beta}(A) - E_{AB}^{\alpha\beta}(B) + E_{AB}^{\alpha}(A) + E_{AB}^{\beta}(B) - E_{A}^{\alpha}(A) - E_{B}^{\beta}(B)$$

$$= \Delta E_{BB} + E_{def}^{\alpha}(A) + E_{def}^{\beta}(B)$$

$$= \Delta E_{uncorr} + [E_{AB}^{\alpha}(A) - E_{AB}^{\alpha\beta}(A)] + [E_{AB}^{\beta}(B) - E_{AB}^{\alpha\beta}(B)] \quad (5)$$

The seven terms on the right-hand side of the first equality can be grouped in two ways in order to (i) emphasize that ΔE_{CP} amounts to adding the deformation energy to ΔE_{BB} and (ii) show that the BSSE correction is carried out separately for each individual fragment, thus highlighting the assumption of additivity underlying the counterpoise correction scheme. Besides, the latter form clearly shows that ΔE_{CP} tends to ΔE since the terms in square brackets vanish at the CBS limit.

Until now, we have considered the formation of a complex from two fragments. Of course, the energetics of reactions involving more fragments (e.g., atomization energy) are also of interest. In these cases, a generalization of the above equations is needed. Two different correction schemes have been proposed which hold for any number N of fragments. In the hierarchical scheme,[38] the interaction energy is decomposed into 1-, 2-, ..., N-body components, and the BSSE is corrected for in each of the components. Unfortunately, the number of independent calculations needed to implement this scheme grows exponentially with N. Turi and Dannenberg[36] proposed a more feasible approach which exploits the additivity assumption by neglecting correction in the 2-, 3-, ..., N-body energy components. The resulting formula is a plain generalization of eq 5 to N fragments:

$$\Delta E_{CP} = E_Z^{\zeta}(Z) - \sum_{k=1}^{N} E_Z^{\zeta}(F_k) + \sum_{k=1}^{N} E_Z^{\varphi_k}(F_k) - \sum_{k=1}^{N} E_{F_k}^{\varphi_k}(F_k) \quad (6)$$

where the fragments F_k ($k = 1, 2, ... N$) with basis set φ_k form the complex Z with basis set $\zeta = \varphi_1 \oplus \varphi_2 \oplus ... \oplus \varphi_N$. For N fragments, ΔE_{CP} can be obtained from $3N + 1$ independent calculations. Note that only the first $2N + 1$ terms on the right side of eq 6 depend on the complex geometry. The number of calculations needed to compute the BSSE correction within the two schemes is reported in Table 1. The two schemes are computationally (and theoretically) equivalent for $N = 2$, but the Turi−Dannenberg scheme enables one to save much computational effort already for $N = 3$, especially when performing PES scans.

TABLE 1: Number *M* of Independent Calculations Needed for BSSE Correction within the Hierarchical and the Turi−Dannenberg Schemes[a]

	$M(P = 1)$		$M(P)$	
N	hierarchical	Turi−Dannenberg	hierarchical	Turi−Dannenberg
2	7	7	$5P + N$	$5P + N$
3	22	10	$19P + N$	$7P + N$
4	129	13	$125P + N$	$9P + N$

[a] N denotes the number of fragments and P the number of structures of the complex one is dealing with, e.g., in a PES scan.

CHART 1. Sketch Representing the Geometry of Complex $H_5O_2^+$ at the Beginning (Top) and toward the End (Bottom) of the Proton Transfer from the Donor (Left) to the Acceptor (Right)[a]

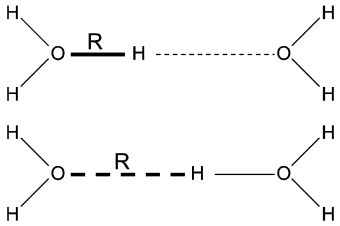

[a] The distance that is fixed during the scan (R) is denoted by a thick line.

Computational Details

As representative systems for proton transfer, we chose HF_2^-, $H_3O_2^-$, $H_5O_2^+$, $N_2H_5^-$, and $N_2H_7^+$, which cover a broad range of relative acidity. As detailed above, we consider these as systems comprising three units: an exchangeable proton and two identical base units (F^-, OH^-, H_2O, NH_2^-, and NH_3, respectively). All computations were carried out at the Hartree−Fock level, followed by second-order Møller−Plesset (MP2) correlation energy correction by the Gaussian98 program suite.[41] Core electrons were frozen at the MP2 step. We carried out calculations employing the following standard basis sets: cc-pVDZ, cc-pVTZ, aug-cc-pVDZ, and aug-cc-pVTZ. Each point on the PES has been obtained by a full geometry optimization, except for the distance R between the heavy atom (F, O, or N) of the donor unit and the exchangeable proton (cf. Chart 1). Such distances have been typically scanned from 0.9 to 2.0 Å (0.025 Å step), thus obtaining a PE curve, i.e., a one-dimensional section of the PES representative of a possible proton exchange from the donor fragment to the acceptor. Clearly, the structural meaning of the fixed distance changes during the scan. For instance, consider the $H_5O_2^+$ system sketched in Chart 1. In the first part of the scan, R is small and we actually fix the length of one of the three O−H bonds within the hydronium ion and optimize all the rest, so that the other fragment (i.e., the water molecule) is fully optimized, including the $H_2OH^+\cdots OH_2$ distance. Conversely, in the last part of the scan, R is large and the first fragment has become a water molecule. Hence, we are now fixing the $H_2O\cdots HOH_2^+$ distance and optimizing all the rest, so that the hydronium ion is fully optimized. This is why the potential energy curves reported below are not symmetrical.

Calculations of the fragments at the complex geometry were performed both with the whole basis set and with the basis set of the fragment itself. Since we are dealing with proton-transfer reactions, we employ a three-fragment formalism where the exchangeable proton is considered an independent entity, as described in the previous section. The fragment choice is trivial: one fragment is the exchangeable proton, and the other two are the identical base units exchanging the proton. Of course, the proton has its own basis set but bears no electron, so the summations in the right member of eq 6 are restricted to

the base units, but the merged basis set does contain the atomic orbitals of the exchangeable proton.

Results and Discussion

We present and discuss first the general characteristics of the PE curve shape for proton transfer, then the details and peculiarities of the individual proton-exchanging complexes. We recall that the scope of this paper is not the accurate energetic and structural characterization of the complexes. In the long run, we are interested in quantum and semiclassical simulations of proton-transfer processes which need large PES scans. These simulations do not require accurate absolute values of the interaction energy, but rather an accurate shape of the PES. Indeed, potential energy curves are usually scaled so that their minimum is the zero of the energy scale. In conclusion, our aim is to answer the following questions: (i) How is the PES shape affected by the basis set choice and the BSSE? (ii) Which basis set is the best compromise between accuracy and computational speed?

General Characteristics of the PE Curve Shape. The PE curves for the studied proton-transfer reactions may exhibit both single- and double-well shape. In the former case, shape analysis is straightforward since it amounts to studying the position of the minimum and the wall slope. For double-well curves, one has to take into account the position of the two minima and the maximum, the barrier height, and the slope of the external repulsive walls.

The basis set choice and the 3fCP correction may, in principle, affect all of the above-mentioned features of the PE shape. With reference to proton exchange between identical base units A and A′, we can define the shape difference as

$$\Delta s = [\Delta E_{\mathrm{CP}} - \min(\Delta E_{\mathrm{CP}})] - [\Delta E_{\mathrm{uncorr}} - \min(\Delta E_{\mathrm{uncorr}})]$$
$$= [E^{\alpha}_{\mathrm{AB}}(\mathrm{A}) - E^{\alpha\beta}_{\mathrm{AB}}(\mathrm{A})] + [E^{\beta}_{\mathrm{AB}}(\mathrm{A}') - E^{\alpha\beta}_{\mathrm{AB}}(\mathrm{A}')] + C \quad (7)$$

where $C = \min(\Delta E_{\mathrm{uncorr}}) - \min(\Delta E_{\mathrm{CP}}) > 0$ is a constant vertical offset, and the terms in square brackets are the contributions of the A and A′ fragments to the counterpoise correction. Note that although the 3fCP correction $\Delta E_{\mathrm{CP}} - \Delta E_{\mathrm{uncorr}}$ is always non-negative, the shape difference may take either sign. Where $\Delta s > 0$, the 3fCP corrected curve lies above the uncorrected one, and vice versa, once the curves have been energetically offset so that their minima are at zero level.

Typical examples of the 3fCP correction as a function of R are shown are Figure 2. The part of the 3fCP correction allotted to the donor fragment monotonically decreases with increasing R since the overlap with the basis functions of the other two fragments and the deformation the latter induces become smaller. Of course, they must vanish for $R \rightarrow \infty$. This curve may be quasi-linear or show concavity toward either higher and lower energy. Such different shapes may be observed even within a single complex with different basis sets. The part of the 3fCP correction allotted to the acceptor fragment monotonically increases with increasing R and is generally concave toward lower energy, except for very short R values in some cases. At variance with the donor fragment contribution, that of the acceptor tends to level off rather early, when the basis set augmentation and the structural deformation effects caused by the presence of the donor fragment become negligible, but it does not vanish for $R \rightarrow \infty$, since the effects due to the nearby proton are still present. This early leveling causes the overall 3fCP correction to have a negative slope for moderately large R and the shape difference Δs to become negative in this region. Therefore, the 3fCP-corrected PE curve shows a minimum with a less steep wall at larger R (or a broader rightmost potential well in the case of double-well curves).

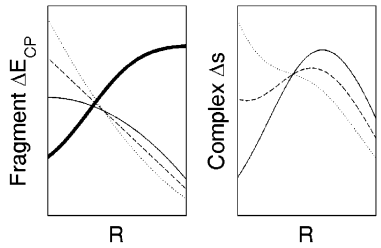

Figure 2. Schematic representation of the three-fragment counterpoise correction of the nonproton fragments and of the proton-exchanging complex. (Left) Contributions from the acceptor (thick line) and the donor (thin lines) base fragment. The latter ones illustrate the three possible concavities observed: concave toward low energy (type I, solid line); quasi-linear (type II, dashed line); and concave toward high energy (type III, dotted line). (Right) The three possible shapes for the counterpoise correction of the proton-exchanging complex obtained as the sum of the fragment contributions shown in the left panel. Each PE curve may possess a single maximum (type I, solid line), a maximum and a minimum (type II, dashed line), or an inflection point (type III, dotted line).

The shape of the donor part of the overall 3fCP correction depends on the details of the fragments 3fCP correction. In the simplest case, the overall 3fCP correction has a maximum near the R value where the complex has a symmetric structure and slopes downward for smaller R (type I). The potential well is thus made broader in the case of single-well curves. For double-well curves, the external walls of both wells are less steep. In other cases, the interplay between the two contributions is such that the 3fCP correction rises at short enough R. The maximum may be followed at shorter R by a minimum (type II), or it may be replaced by an inflection point (type III), usually near the symmetric structure. In this case, Δs is bound to become positive at short R, and there the potential well becomes more repulsive.

The behavior of Δs in the central R range depends on the interplay of many factors. However, in most cases a maximum in Δs is observed in this range, leading to well broadening in the single-well case and to higher barriers in the double-well case. If an inflection point is present, the 3fCP-corrected curve is more asymmetric than the uncorrected one.

The [F···H···F]$^-$ Complex. In this case, all fragments are atomic in nature, so the deformation energy vanishes and $\Delta E_{\mathrm{CP}} = \Delta E_{\mathrm{BB}}$. The PE curves and Δs for the [F···H···F]$^-$ complex computed with the cc-pVDZ, cc-pVTZ, aug-cc-pVDZ, and aug-cc-pVTZ basis sets are shown in Figure 3. All the uncorrected curves show a single minimum at $R_0 = 1.150$ Å, corresponding to a symmetrical structure, but differ in the width of the well, the two aug-cc curves having a less steep walls. The shape difference is of type I for cc basis sets. In these cases, $\Delta s < 0$ except for a narrow range about $R = R_0$, so the potential well is made broader on either side. For the aug-cc sets, type III is observed and $\Delta s > 0$ for $R < R_0$, so the potential well is broader at large R but slightly steeper at small R. Notwithstanding the actual 3fCP correction is largely different between augmented and nonaugmented basis sets (this is an anionic system), Δs is small and not very different among the four basis sets. As to the relative shape of the corrected PE curves, we see a behavior similar to that of the uncorrected ones; namely, they present a single minimum, and the aug-cc-pVDZ and aug-cc-pVTZ results show less steep walls on both sides of the well than their cc-pVDZ and cc-pVTZ counterparts. For instance, the difference between the offset cc-pVDZ and aug-cc-pVDZ amounts to about 1.3 kcal/mol at $R = 1.4$ Å. From the relative accuracy of the

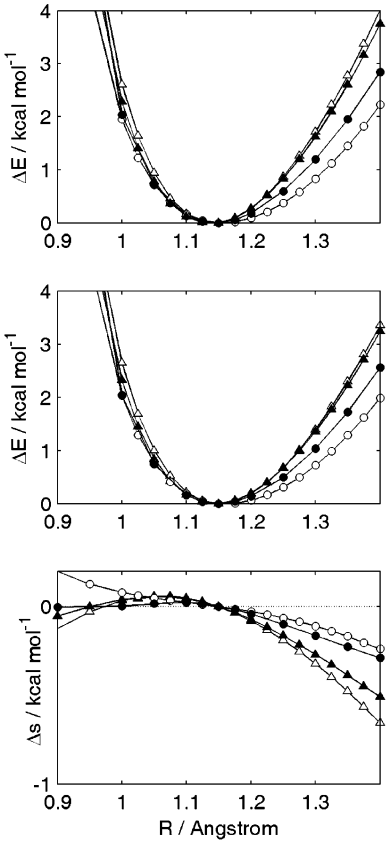

Figure 3. Shape difference and comparison between the potential energy curves for the $[F\cdots H\cdots F]^-$ complex computed with four basis sets. (Top) Uncorrected PE curves; (middle) 3fCP-corrected PE curves; (bottom) shape differences. △, cc-pVDZ; ▲, cc-pVTZ; ○, aug-cc-pVDZ; ●, aug-cc-pVTZ.

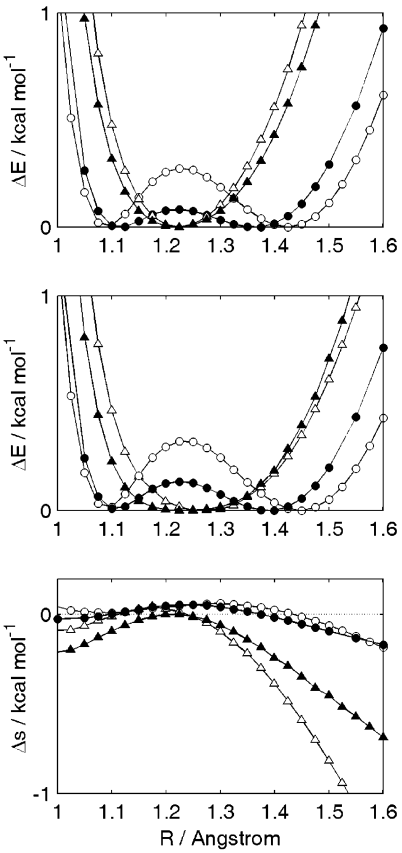

Figure 4. Shape difference and comparison between the potential energy curves for the $[HO\cdots H\cdots OH]^-$ complex computed with four basis sets. (Top) Uncorrected PE curves; (middle) 3fCP-corrected PE curves; (bottom) shape differences. △, cc-pVDZ; ▲, cc-pVTZ; ○, aug-cc-pVDZ; ●, aug-cc-pVTZ.

corrected curves, we can say that, for a large PES scan, one should at least use the largest basis set employed in this work.

The $[HO\cdots H\cdots OH]^-$ Complex. In this system, the deformation energy is due simply to the change in the O−H bond length within the hydroxyl ions. In Figure 4, the PE curves computed with the four basis sets along with the correspondent Δs are reported. Interestingly, the necessity of using basis sets containing diffuse functions to correctly describe an anionic system shows itself off by inducing dramatic differences in the topology of the proton-transfer PE curve for this complex. Whereas the two uncorrected aug-cc PE curves present a double-well potential (saddle at 1.225 Å), their cc counterparts predict a single-well PE curve, with their minima located at 1.250 (cc-pVDZ) and 1.225 Å (cc-pVTZ), respectively. The position of the two minima of the aug-cc PE curves strongly depends on the quality of the basis set. Specifically, the aug-cc-pVDZ minima are located at shorter and longer distances than the aug-cc-pVTZ ones when the proton is bound to the donor and to the acceptor, respectively. Also, the barrier height (see Table 2) decreases by roughly 0.19 kcal/mol on going from aug-cc-pVDZ (0.27 kcal/mol) to aug-cc-pVTZ (0.08 kcal/mol). A similar behavior is found for the corrected PES, the corrected barrier height decreasing from 0.32 to 0.13 kcal/mol, and the location of the minima becoming closer. The shape difference is of the type II for all the computed PE curves. Whereas for the two aug-cc sets $\Delta s > 0$ for $R < 1.4$ and $\Delta s < 0$ for larger R, such that the barrier is increased and the steepness of the walls decreased, the two cc sets present a very small shape difference in the regions around their minima. We notice that the shape difference for the augmented basis sets introduces small changes in the location of the two minima, displacing them to larger R in both cases. This effect appears to be more important for the smallest basis set. We also notice that the BB correction scheme (data not shown) is in quite good agreement with the full 3fCP correction for this system. As to the total accuracy of the corrected PE curves, from our results it seems that the aug-cc-pVDZ basis set is not flexible enough to allow a total accuracy of, at least, 0.1 kcal/mol for this system, and that the aug-cc-pVTZ or larger sets should be used.

TABLE 2: Uncorrected and 3fCP-Corrected Barrier Heights (kcal/mol^{-1}) for the Proton Transfer in the $H_3O_2^-$, $N_2H_5^-$, and $N_2H_7^+$ Systems for the Four Employed Basis Sets[a]

system	correction scheme	cc-pVDZ	cc-pVTZ	aug-cc-pVDZ	aug-cc-pVTZ
$H_3O_2^-$	none			0.27	0.08
	3fCP			0.32	0.13
$N_2H_7^+$	none	0.41	0.64	0.96	0.72
	3fCP	0.94	0.94	1.02	0.89
$N_2H_5^-$	none	1.20	1.75	3.90	3.80
	3fCP	2.56	2.72	4.46	4.32

[a] The HF_2^- and $H_5O_2^+$ systems show single-well potential.

The $[H_2O\cdots H\cdots OH_2]^+$ Complex. In this system, three degrees of freedom for each fragment are involved in the relaxation process during the proton exchange. Figure 5 shows the PE curves and Δs for this complex. From this picture, it can be seen that all the PE curves have only a single well, a feature that it is shared also with higher levels of theory, e.g., MP4[10] and CCSD(T),[30] when large basis sets are used. All the minima are located around $R_0 = 1.2$ Å. However, the uncor-

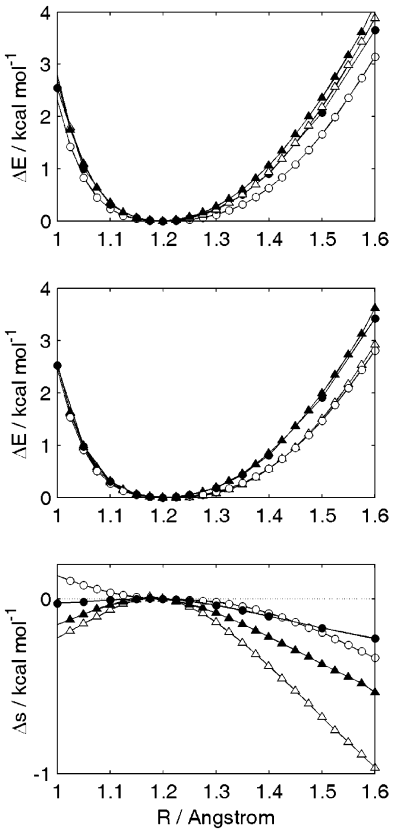

Figure 5. Shape difference and comparison between the potential energy curves for the $[H_2O\cdots H\cdots OH_2]^+$ complex computed with four basis sets. (Top) Uncorrected PE curves; (middle) 3fCP-corrected PE curves; (bottom) shape differences. △, cc-pVDZ; ▲, cc-pVTZ; ○, aug-cc-pVDZ; ●, aug-cc-pVTZ.

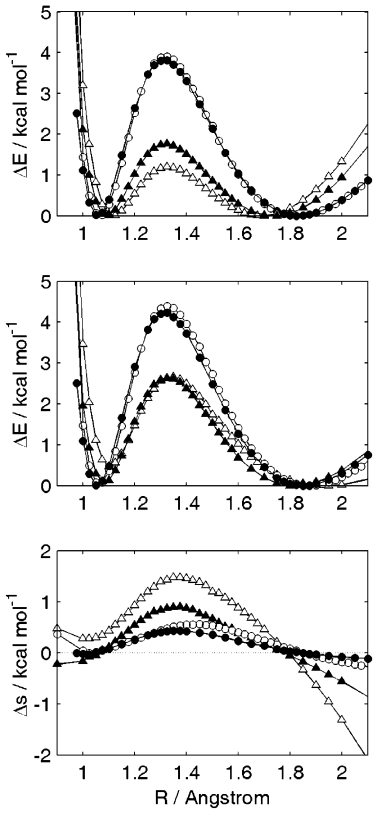

Figure 6. Shape difference and comparison between the potential energy curves for the $[H_2N\cdots H\cdots NH_2]^-$ complex computed with four basis sets. (Top) Uncorrected PE curves; (middle) 3fCP-corrected PE curves; bottom, shape differences. △, cc-pVDZ; ▲, cc-pVTZ; ○, aug-cc-pVDZ; ●, aug-cc-pVTZ.

rected PE curve show different curvatures depending on the basis set employed, with a tendency for the aug-cc-pVDZ results to show less steep walls than the results for the other basis sets. Although the main features do not change after the 3fCP correction, a better agreement between cc-pVDZ and aug-cc-pVDZ basis sets is found. A similar outcome is found also for the cc-pVTZ/aug-cc-pVTZ pair. Therefore, in this cationic system, the 3fCP scheme can correct for the absence of diffuse functions but not for that of an additional ζ subset. The shape difference is of type III for the aug-cc-pVDZ set and of type II for the other ones. Hence, $\Delta s > 0$ only for the aug-cc-pVDZ set and for $R < R_0$. The BB- and 3fCP-corrected curves are in good agreement in the region around the potential minimum, while they diverge at both small and large values of R. As to the overall accuracy of the 3fCP-corrected surfaces (see Figure 5), although the four PE curves are in good agreement with respect to the position of the minimum of the potential with a relative discrepancy better than 0.025 Å, our results clearly indicate that the DZ quality basis sets are not flexible enough to describe the walls of the well with an accuracy better than 0.1 kcal/mol. Conversely, the good agreement between of the two TZ basis sets after the 3fCP correction, together with the results shown in refs 10 and 30, indicates that the cc-pVTZ set could give an accurate description of the proton-exchange surface for this complex.

The $[H_2N\cdots H\cdots NH_2]^-$ Complex. The NH_2^- fragments of this complex present the largest proton affinity, and hence the strongest basic behavior, among all the systems we studied. Figure 6 shows PE curves and Δs for this system. All of the uncorrected PE curves clearly show a double-well interaction potential. However, they present large differences in both the location of the minima at larger R and the barrier heights between the two aug-cc and the two cc sets (see Figure 6). The former basis sets give very close barrier heights (3.90 and 3.81 kcal/mol), whereas the cc sets are much lower and also more dispersed (1.20 and 1.75 kcal/mol). The shape difference appears to be of type II for every basis set. Obviously, this increases the barrier height and decreases the steepness of the repulsive potential wall at large R. Besides, the absolute value of Δs strongly depends on the basis set, the aug-cc sets being those requiring the smallest overall correction. As for the relative accuracy of the 3fCP-corrected PE curves, from Figure 6 one can see that the curves are close to each other and that the locations of the minima are much less dependent on the basis set. An interesting point is the raising of the minimum at small R relative to that at large R and the shift of the latter to larger R induced by the 3fCP correction on the PE curve from cc basis sets. Both effects are not present in the correction of aug-cc PE curves, and so they can be regarded as artifacts. As for the barrier heights, the 3fCP correction has a large beneficial effect on the values from the cc basis sets, which turn out to be closer and larger by more than ~1 kcal/mol. The aug-cc barriers are again close to each other and about 0.5 kcal/mol higher with respect to the uncorrected values. Although introducing the BSSE corrections improves the agreement between the two different groups of results, the results still show marked differences, especially in the barrier heights. This finding indicates once more that the absence of diffuse functions can introduce a strong bias when dealing with anionic systems, such that even the 3fCP approach cannot fully account for this absence. Conversely, the 3fCP correction is able to countervail the different number of ζ subsets, in contrast to the behavior observed with $H_5O_2^+$. Hence, a 2D scan of the proton-transfer

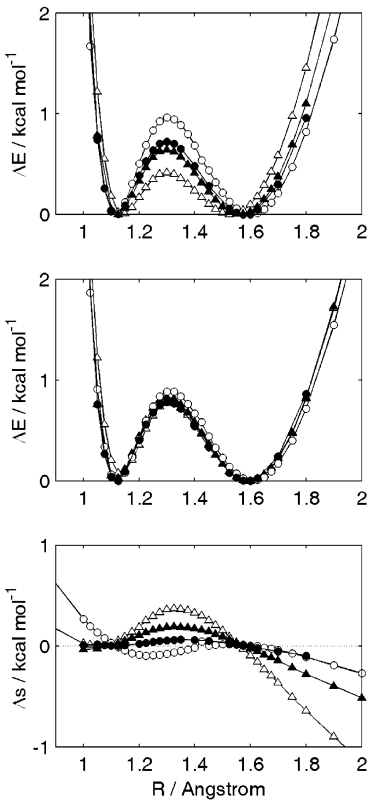

Figure 7. Shape difference and comparison between the potential energy curves for the $[H_3N\cdots H\cdots NH_3]^+$ complex computed with four basis sets. (Top) Uncorrected PE curves; (middle) 3fCP-corrected PE curves; (bottom) shape differences. △, cc-pVDZ; ▲, cc-pVTZ; ○, aug-cc-pVDZ; ●, aug-cc-pVTZ.

PES for this complex could be carried out by employing the aug-cc-pVDZ atomic basis set. From the dynamical point of view, this complex seems to be the best candidate to study the coupling between the proton motion along the N−N internuclear axis and the N−N vibrational motion. Indeed, the high barrier and its decrease upon a fragment approaching may force a "corner cutting" on the propagated wave packet around the barrier itself. The relative importance of this effect should depend strongly on the overall topology of the computed PES in the saddle point region.

The $[H_3N\cdots H\cdots NH_3]^+$ Complex. Among the complexes we studied in this work, this is the system that possess the largest number of internal degrees of freedom for each of the two fragments, i.e., 6. In Figure 7, we show the PE curve and Δs computed using the four basis sets. Similarly to the $N_2H_5^-$ case, all of the four uncorrected PE curves show a double-well interaction potential. Notwithstanding this similarity, the dependency of both the location of the right minimum (i.e., large R and proton bound to the right fragment) and the height of the potential barrier on the quality of the basis set is large. The position of the minimum spans the distance range 1.525−1.600 Å, and the height of the barrier varies from 0.41 to 0.96 kcal/mol as an effect of the quality of the basis set (see Table 2). This dependency is largely reduced by correcting the PE curve for the BSSE by using eq 7, as clearly seen in Figure 7, so the equilibrium distances differ by less than 0.025 Å, and the barriers are all within the range of 0.12 kcal/mol. The shape difference appears to be of type II for all the basis sets used in this work, showing positive values in the region between the two minima (hence increasing the barrier) and a negative sign for $R > 1.55$ Å. Interestingly, the BB correction seems to overestimate the 3fCP one by 0.1−0.2 kcal/mol in the region between the two minima for all the basis sets. This effect is obviously due to the deformation energy, and it is expected to produce a barrier that is too large with respect to the CBS limit. As to the relative accuracy of the four PE curve, our results show that, if one is interested in having an accuracy of 0.1 kcal/mol for the barrier height and of 0.02 Å on the geometry of the minima after BSSE correction, all the basis sets seems to be equally effective. For $N_2H_5^-$, raising of the minimum at small R is observed, even if the effect is smaller in the present case. However, this shows that augmented basis sets are mandatory to study even this cationic system. Although the aug-cc-pVDZ results slightly overestimate the barrier to proton transfer by about 0.1 kcal/mol, we advise to consider its use for PE curve production purposes since the aug-cc-pVTZ basis set is computationally very expensive for a fully relaxed PES scan.

Conclusions

The most general conclusion to draw on the basis of the above results is that the effects of basis set choice and of 3fCP correction are strongly system dependent and therefore should be studied separately for each system under consideration. The topology of the PE curve, i.e., the number of maxima and minima, is mainly determined by the system itself. Indeed, a double-well potential is found with more basic fragments. However, a case was found, namely $[HO\cdots H\cdots OH]^-$, where the topology strongly depends on the basis set. The choice of the latter also affects the parameters quantitatively describing the PE curve, that is, the location and relative energy of maxima and minima. Larger effects are observed in the uncorrected PE curves of systems comprising more basic fragments.

The difference between the BB and the 3fCP correction (i.e., the deformation energy) grows with the number of internal degrees of freedom of the fragments, as expected. The 3fCP correction does not affect the PE curve topology, but it may affect the parameters in the sense that the differences among parameters computed with different basis sets may be partially or almost completely suppressed. It was most effective for the $H_5O_2^+$, $N_2H_5^-$, and above all $N_2H_7^+$ systems but was much less beneficial for $H_3O_2^-$ and HF_2^-. Therefore, larger differences are corrected for when electronically less rigid fragments are involved. Hence, a general trend can be delineated: the effect of basis set incompleteness and the counteracting correction of the BSSE follow the trend F < O < N.

Finally, we give some hints about the best-compromise basis set for computing extensive PES. For $N_2H_7^+$ and $N_2H_5^-$, the aug-cc-pVDZ set seems to be adequate if one is satisfied with a 0.1 kcal/mol = 35 cm^{-1} accuracy. This basis set can also be used with $H_3O_2^-$ if an accuracy of 0.2 kcal/mol is acceptable; otherwise, the much larger aug-cc-pVTZ is needed. Notwithstanding its simplicity, the HF_2^- system apparently needs the aug-cc-pVTZ set because the aug-cc-pVDZ-corrected energy differs from the latter by more than 0.1 kcal/mol already at 0.05 Å from the minimum. Conversely, the cc-pVTZ basis set seems to give the overall best accuracy/cost ratio for the $H_5O_2^+$ system when supplemented by the 3fCP correction procedure, so we suggest its use for scanning the potential energy surface of protonated water clusters.

References and Notes

(1) Alonso, D. O. V.; DeArmond, S.; Cohen, F.; Daggett, V. *Proc. Natl. Acad. Sci. U.S.A.* **2001**, *98*, 2985.

(2) Fersht, A. R. *Structure and Mechanism in Protein Science: A Guide to Enzyme Catalysis and Protein Folding*; W. H. Freeman & Co.: New York, 1999.

(3) Bakker, H. J.; Nienhuys, H. K. *Science* **2002**, *297*, 587.

(4) Alfano, D.; Borrelli, R.; Peluso, A. *J. Phys. Chem. A* **2002**, *106*, 7018.
(5) Heller, E. J. *J. Phys. Chem.* **1995**, *99*, 2625.
(6) Marx, D.; Tuckerman, M. E.; Hutter, J.; Parrinello, M. *Nature* **1999**, *397*, 601.
(7) Liu, Y.; Tuckerman, M. E. *J. Phys. Chem. B* **2001**, *105*, 6598.
(8) Tuckerman, M. E.; Marx, D.; Parrinello, M. *Nature* **2002**, *417*, 925.
(9) Aqvist, J.; Warshel, A. *Chem. Rev.* **1993**, *93*, 2523.
(10) Ojamae, L.; Shavitt, I.; Singer, S. J. *J. Chem. Phys.* **1998**, *109*, 5547.
(11) Day, T. J. F.; Soudackov, A. V.; Cuma, M.; Schmitt, U. W.; Voth, G. A. *J. Chem. Phys.* **2002**, *117*, 5839.
(12) Boys, S. F.; Bernardi, F. *Mol. Phys.* **1970**, *19*, 553.
(13) van Duijneveldt, F. B.; van Duijneveldt-van de Rijdt, J. G. C. M.; van Lenthe, J. H. *Chem. Rev.* **1994**, *94*, 1873.
(14) Simon, S.; Duran, M.; Dannenberg, J. J. *J. Chem. Phys.* **1996**, *105*, 11024.
(15) Xantheas, S. S. *J. Chem. Phys.* **1996**, *104*, 8821.
(16) Salvador, P.; Duran, M.; Dannenberg, J. J. *J. Phys. Chem.* **2002**, *106*, 6883.
(17) Kobko, N.; Dannenberg, J. J. *J. Phys. Chem.* **2001**, *105*, 1944.
(18) Yamashita, K.; Morokuma, K.; Leforestier, C. *J. Chem. Phys.* **1993**, *99*, 8848.
(19) Platts, J. A.; Laidig, K. E. *J. Phys. Chem.* **1996**, *100*, 13455.
(20) McAllister, M. A. *Theochem* **1998**, *427*, 39.
(21) Perera, S. A.; Bartlett, R. J. *J. Am. Chem. Soc.* **2000**, *122*, 1231.
(22) Kawahara, S.; Uchimaru, T.; Taira, K. *Chem. Phys.* **2001**, *273*, 207.
(23) Xantheas, S. S. *J. Am. Chem. Soc.* **1995**, *117*, 10373.
(24) Pliego, J. R.; Riveros, J. M. *J. Phys. Chem.* **2000**, *104*, 5155.
(25) Pliego, J. R.; Riveros, J. M. *J. Chem. Phys.* **2000**, *112*, 4045.
(26) Brodskaya, E.; Lyubartsev, A. P.; Laaksonen, A. *J. Phys. Chem.* **2002**, *106*, 6479.
(27) Masamura, M. *J. Chem. Phys.* **2002**, *117*, 5257.
(28) Xie, Y.; Remington, R. B.; Shaefer, H. F., III. *J. Chem. Phys.* **1994**, *101*, 4878.
(29) Kar, T.; Scheiner, S. *Int. J. Quantum Chem. Symp. Ser*. **1995**, *29*, 567.
(30) Valeev, E. F.; Shaefer, H. F., III. *J. Chem. Phys.* **1999**, *108*, 7197.
(31) Hodges, M. P.; Stone, A. J. *J. Chem. Phys.* **1999**, *110*, 6766.
(32) Roszak, S. *J. Chem. Phys.* **1996**, *105*, 7569.
(33) Asada, T.; Haraguchi, H.; Kitaura, K. *J. Phys. Chem. A* **2001**, *105*, 7423.
(34) Meuwly, M.; Karplus, M. *J. Chem. Phys.* **2002**, *116*, 2572.
(35) Wang, B. C.; Chang, J. C.; Jiang, J. C.; Lin, S. H. *Chem. Phys.* **2002**, *276*, 93.
(36) Turi, L.; Dannenberg, J. J. *J. Phys. Chem.* **1993**, *97*, 2488.
(37) Mayer, I.; Surján, P. R. *Chem. Phys. Lett.* **1992**, *191*, 497.
(38) Lendvay, G.; Mayer, I. *Chem. Phys. Lett.* **1998**, *297*, 365.
(39) Simon, S.; Duran, M.; Dannenberg, J. J. *J. Phys. Chem. A* **1999**, *103*, 1640.
(40) Salvador, P.; Duran, M. *J. Chem. Phys.* **1999**, *111*, 4460.
(41) Frisch, M. J.; Trucks, G. W.; Schlegel, H. B.; Scuseria, G. E.; Robb, M. A.; Cheeseman, J. R.; Zakrzewski, V. G.; J. A. Montgomery, J.; Stratmann, R. E.; Burant, J. C.; Dapprich, S.; Millam, J. M.; Daniels, A. D.; Kudin, K. N.; Strain, M. C.; Farkas, O.; Tomasi, J.; Barone, V.; Cossi, M.; Cammi, R.; Mennucci, B.; Pomelli, C.; Adamo, C.; Clifford, S.; Ochterski, J.; Petersson, G. A.; Ayala, P. Y.; Cui, Q.; Morokuma, K.; Rega, N.; Salvador, P.; Dannenberg, J. J.; Malick, D. K.; Rabuck, A. D.; Raghavachari, K.; Foresman, J. B.; Cioslowski, J.; Ortiz, J. V.; Baboul, A. G.; Stefanov, B. B.; Liu, G.; Liashenko, A.; Piskorz, P.; Komaromi, I.; Gomperts, R.; Martin, R. L.; Fox, D. J.; Keith, T.; Al-Laham, M. A.; Peng, C. Y.; Nanayakkara, A.; Challacombe, M.; Gill, P. M. W.; Johnson, B.; Chen, W.; Wong, M. W.; Andres, J. L.; Gonzalez, C.; Head-Gordon, M.; Replogle, E. S.; Pople, J. A. *Gaussian 98*, Revision A.11.3; Gaussian, Inc.: Pittsburgh, PA, 2002.